International Journal of Earth, Energy and Environmental Sciences
ISSN: 2517-942X
Vol:9, No:6, 2015

Optimization of a Four-Lobed Swirl Pipe for Clean-In-Place Procedures

Guozhen Li, Philip Hall, Nick Miles, Tao Wu

***Abstract*—**This paper presents a numerical investigation of two horizontally mounted four-lobed swirl pipes in terms of swirl induction effectiveness into flows passing through them. The swirl flows induced by the two swirl pipes have the potential to improve the efficiency of Clean-In-Place procedures in a closed processing system by local intensification of hydrodynamic impact on the internal pipe surface. Pressure losses, swirl development within the two swirl pipe, swirl induction effectiveness, swirl decay and wall shear stress variation downstream of two swirl pipes are analyzed and compared. It was found that a shorter length of swirl inducing pipe used in joint with transition pipes is more effective in swirl induction than when a longer one is used, in that it has a less constraint to the induced swirl and results in slightly higher swirl intensity just downstream of it with the expense of a smaller pressure loss. The wall shear stress downstream of the shorter swirl pipe is also slightly larger than that downstream of the longer swirl pipe due to the slightly higher swirl intensity induced by the shorter swirl pipe. The advantage of the shorter swirl pipe in terms of swirl induction is more significant in flows with a larger Reynolds Number.

***Keywords*—**Swirl pipe, swirl effectiveness, CFD, wall shear stress, swirl intensity.

I. Introduction

INDUSTRIES such as dairy, beverage, brewing, processed foods, pharmaceutical, and cosmetics rely heavily on Clean-In-Place (CIP) procedures to frequently clean their production lines. A CIP procedure is a method of cleaning the interior surfaces of pipes, vessels, process equipment and associated fittings, without disassembling them. The benefit to industries by using CIP is that the cleaning is faster, less labor intensive, more repeatable, and poses less chemical exposure risks to people. Efficient CIP is important to maintain good operation of the production line and more importantly to ensure the appropriate level of hygiene and thus the safety of the products [1], [2]. Efficient CIP will result not only in reduced downtime and costs for cleaning but also decreased environmental impact (in the disposal of spent chemicals) [3].

CIP is usually performed by the circulation of formulated detergents which typically involves a warm water rinse, washing with alkaline and/or acidic solution, and a clear rinse with warm water to flush out residual cleaning agents [4]. Research established that the CIP efficiency depends on mainly four energy factors: the chemical action from detergents to dissolve soil in order to facilitate removal, the thermal energy - the cleaning temperature, the cleaning time, and the favorable mechanical energy (or hydrodynamic effect) to physically remove soil [2], [5]-[8]. An efficient combination of those factors varies depending on the type of soil and the severity of the fouling and a restriction in one factor may be compensated by increasing the effect of one or more of others [5]. Literature showed that, of the hydrodynamic factors, the wall shear stress, which is a measure of the mechanical action of fluid flow on a process surface, is considered the dominating factor for cleaning. The effective removal rate is significantly influenced by the wall shear stress applied during cleaning [1], [5], [9].

Lately we proposed a method to improve the CIP efficiency by introducing swirl motion into CIP flow which should intensify the hydrodynamic effect of cleaning fluid to physically remove the soil. We have numerically identified the potential of a geometrically induced swirl flow generated from flow passing through a four-lobed swirl pipe (600mm in length, 50mm in diameter) on improving the CIP efficiency by locally increasing the mean shear stress at the internal pipe surface without increasing the overall flow velocity [10]. The Computational Fluid Dynamics (CFD) model showed that the 600 length four-lobed swirl pipe imparted a tangential wall shear stress to the swirl flow downstream of it which is proportional to the swirl intensity of the swirl flow induced. As a result of the presence of tangential wall shear stress, the mean wall shear stress downstream of the swirl pipe was increased.

However, it was found that the pressure loss across the four-lobed swirl pipe is more significant than that of the circular pipes, which is due to the additional turbulence generated through the artificial roughness of the non-circular pipe cross-sections of the swirl pipe. This paper intends to further optimize the 600mm length four-lobed swirl pipe by shortening its length to 400mm. This should further decrease the extra pressure loss expended in inducting swirl into flow passing through the swirl pipe. A criterion based on the ratio of the swirl intensity produced to the pressure loss was used to calculate the swirl effectiveness of the two swirl pipes. The pressure losses across the 600mm and 400mm swirl pipes, the swirl development within the two swirl pipes, their swirl effectiveness, swirl decay and wall shear stress variation downstream of two swirl pipes were analyzed and compared.

Guozhen Li, Nick Miles, and Tao Wu are with the University of Nottingham Ningbo China, 199 Taikang East Road, Ningbo, 315100, China (e-mail: Guozhen.LI@nottingham.edu.cn, Nick.Miles@nottingham.edu.cn, Tao.Wu@nottingham.edu.cn).

Philip Hall is with the University of Nottingham Ningbo China, 199 Taikang East Road, Ningbo, 315100, China (corresponding author; phone: +86(0)574 8818 0018; e-mail: Philip.Hall@nottingham.edu.cn).

II. The 600mm Length and 400mm Length Four-Lobed Swirl Pipes

Swirl flow is one of the well-recognized configurations of the flow in the industrial equipment and is accentuated for its various applications as well as its sophisticated scientific basis [11]. At the University of Nottingham, researches into method to generate swirl flow using helically formed pipes have been carried out for many years. Early emphasis concentrated on the physical effects of swirl section, later research was directed toward optimizing the swirl configuration, number of lobes, pitch to diameter ratio and so on. Ganeshalingam [12] tested various cross-sections of pipe (3, 4, 5 and 6 lobed) and concluded that a 4-lobed cross-section was most effective at swirl generation. The evaluation criteria was the Swirl Effectiveness which was deemed to be the swirl intensity that could be induced for a given pressure drop. He recommended a P:D ratio of 8 and 400mm of length as optimal for the 4-lobed pipe. Pitch is the axial distance travelled by the each lobe as it rotates through 360 degrees (Singh, 1976), therefore a pitch to diameter (P:D) ratio of 8 indicates that the lobed cross-section rotates by 360 degrees (one swirl) in a length equivalent to 8 diameters. The swirl inducing pipe, as shown in Fig. 1, has an equivalent cross-sectional area to the circular pipe delivering fluid to the swirl pipe and the swirl pipe has an 'equivalent' diameter of 50mm.

Fig. 1 Swirl inducing pipe, 400mm length, P:D=8

It was found that there were high entry and exit pressure losses across this swirl inducing pipe due to the sudden change in cross-section from lobed to circular and vice versa. Transition geometries prior to and after the swirl pipe were suggested to eliminate these pressure losses. This should further improve the applicability of the swirl inducing pipes. However the transition section would have to be short and effective. Otherwise it will increase overall pressure drop and, in the case of exit transition, may decrease swirl intensity.

Ariyaratne [13] designed and optimized a transition pipe for use as an entry and exit duct with the swirl inducing pipe. It was found that transition pipes either before or after the swirl inducing pipe reduced entry and exit pressure losses by providing a gradual transition from circular to lobed cross-section and vice versa. They also increased induced swirl and reduced swirl decay. As shown in Fig. 2, the transition pipe's cross-section changes from circular to 4-lobed shape gradually. The area of the cross-sections is constant and equal to the swirl pipe's. The length of transition pipe is 100mm, and each lobe rotates by 90°.

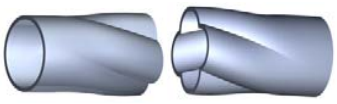

Fig. 2 Entry and exit transition pipes, 100mm length

Based on the study of Ariyaratne, a swirl pipe configuration of 100mm transition pipe prior + 400mm swirl inducing pipe + 100 transition pipe after (as shown in Fig. 3) is deemed to be optimum, which is demonstrated in Fig. 3. However, in this configuration:

- The swirl pipe has the lobed cross-section rotated by 540º (one and a half swirl) instead of 360 º (one swirl), which was used in the previous designs.
- The longer swirl pipe results in more pressure loss due to the increase in contact area and thus friction.
- When entry transition pipe was used in conjunction with swirl pipe, a higher tangential velocity was generated. However, the induced swirl appeared to be constrained by the swirl pipe inducing pipe geometry. A shorter length of swirl inducing pipe will therefore be required to generate an equivalent amount of swirl [13].

Ariyaratne [13] suggested that, with the inclusion of transitions, a shorter length of swirl inducing pipe than previously determined is optimum. Therefore we propose a swirl pipe configuration of 100mm transition pipe prior + 200mm swirl inducing pipe + 100 transition pipe after. This configuration has one swirl, shorter length, and is expected to be more cost effective in swirl induction.

We will numerically compare the two swirl pipe configuration in terms of pressure cost, swirl intensity, swirl effectiveness, swirl decay rate, and the shear stress of swirl flow acted on the pipe surface induced by them as we intend to apply the swirl pipe into pipe cleaning industries where the wall shear stress was reported to be the governing factor in the Clean-In-Place procedures [1].

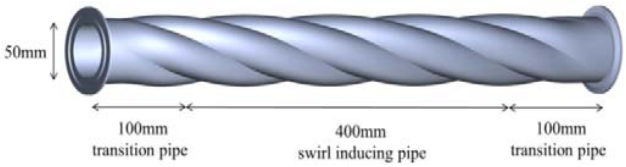

Fig. 3 100+400+100 swirl pipe, 600mm length, one and a half swirl

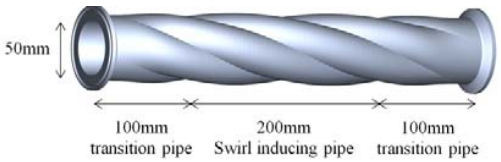

Fig. 4 100+200+100 swirl pipe, 400mm length, one swirl

III. Terms and Definitions

This section introduces a number of terms and equations that will be used in this paper.

A. Swirl Effectiveness

Ganeshalingam [12] defined a Swirl Effectiveness parameter, based on the ratio of the swirl intensity produced to the pressure loss, and used it in all swirl effectiveness calculations. The effectiveness of swirl induction was deemed to be the swirl intensity that could be induced for a given pressure drop. This parameter is also used in this research for

the comparison of the two swirl pipe configurations in terms of swirl effectiveness.

$$Swirl\ Effectiveness = \frac{Swirl\ Intensity}{\frac{\Delta P}{\frac{\rho \times u^2}{2}}} \quad (1)$$

where ΔP is pressure drop, ρ is density, and u is flow velocity.

B. Swirl Intensity and Its Decay Rate

Swirl intensity or swirl number, S, is commonly used to quantify the degree or strength of a swirl within a pipe. This non-dimensional number is defined as the ratio of the angular momentum flux to the axial momentum flux, multiplied by the hydraulic radius [14]. A widely accepted expression of the swirl intensity is given by [15]:

$$S = \frac{\int_0^R uwr^2.dr}{R\int_0^R u^2 r.dr} \quad (2)$$

where w is the tangential velocity, m/s; u is the axial velocity, m/s; r is the radius at the point where tangential velocity is calculated, m; R is the pipe radius, m.

The decay process is quantified by expressing the swirl intensity S as a function of stream wise position x. In most references, the observed swirl intensities are fitted with exponential decay functions

$$S = S_0 e^{-\beta \frac{x}{D}} \quad (3)$$

where β is the decay rate, S_0 is the initial swirl intensity and D is the pipe diameter. The swirl decay rate $\beta = a \times f'$, where a is the empirically or numerically determined coefficient, f' is the Moody friction factor.

C. Tangential Wall Shear Stress

The expression for tangential wall shear stress was derived by Kitoh by treatment of the Reynolds averaged angular momentum equation for incompressible, stationary and axially symmetric flow [14]. The equation later was used by [15] and [11]. For a detailed introduction of tangential wall shear stress and the non-dimensional tangential wall shear stress please refer to [10]. Steenbergen and Voskamp concluded that the existence of tangential wall shear stress in the swirl flow causes reduction of fluid flow swirl intensity [15].

IV. Numerical Method and Models

A. Flow Domain

Configuration of the two modelled pipe flow systems for use with FLUENT academic code [16] is shown in Fig. 5. The 2m straight circular pipes prior to the swirl pipes serve as development section to ensure the flow is fully developed before entering the swirl pipe. The 8m straight circular pipes downstream of the swirl pipes are the test section. The circular pipe has a diameter of 50mm; the swirl pipe has an equivalent diameter of 50mm and its cross-sectional areas are constant and equal to the circular pipe.

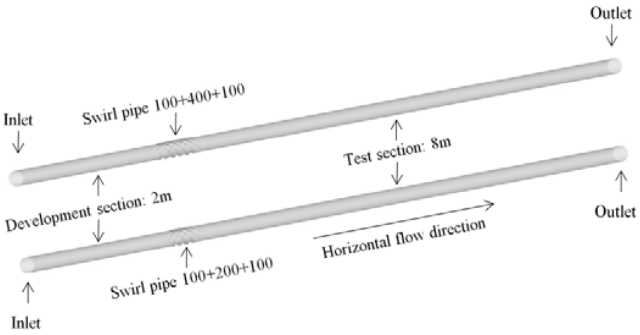

Fig. 5 Configuration of simulation geometry

B. Meshing

Shear stress acting on the pipe wall is of interest in this study, and when an accurate prediction of stress in the boundary layer is required, the boundary layer meshes should consist of quads, hexes, or prisms, and the use of pyramid or tetrahedral cells immediately adjacent to the wall should be avoided [17]. ICEM CFD (ANSYS, USA) mesh generation software was used to mesh the computational domain with structured hexahedral cells. ICEM CFD uses a primarily top-down blocking approach to efficiently mesh complex models using all hexahedral cells without the need to subdivide the geometry. The blocking can be associated with topologically similar geometries. To make sure the blocks in accordance with swirl pipes are well fitted, the blocks are rotated by 45° by moving vertexes of the blocks. O-grid blocks are used to improve overall mesh quality. The cross sectional view of the circular, transition, swirl pipe mashes and the surface mesh of a swirl pipe section are demonstrated in Figs. 6 (a)-(c).

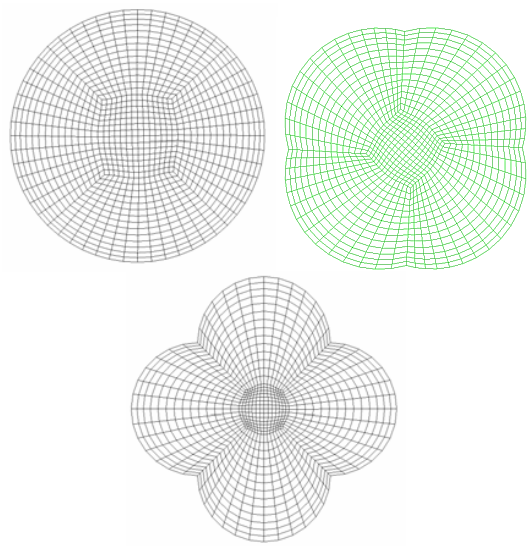

Fig. 6 (a) Cross sectional view of the circular, transition and swirl pipe mashes

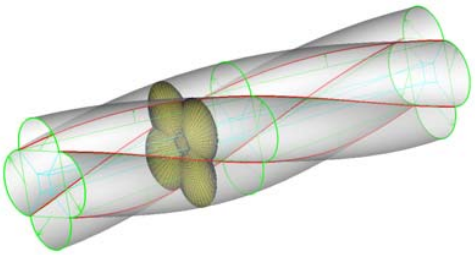

Fig. 6 (b) Association between blocks and geometry

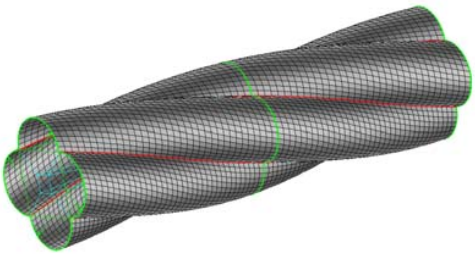

Fig. 6 (c) Surface mesh at the intersection of lobes

Mesh adaption for Non-Equilibrium wall functions was carried out to make sure that the first point where the velocity is calculated is in the log-law region. To ensure that the errors associated with the size of mesh were minimized, a quick mesh independence test was carried out. The detailed process of mesh adaption for wall functions and mesh independence test are described in [10].

C. Numerical Model Description

The governing equations required to predict the flow patterns for the incompressible, single phase, turbulent, swirling flow in the straight and swirl pipe are termed the 'Navier-Stokes Equations'. They are the conservation of mass, momentum and energy. The conservation of energy was not used in the current simulation since heat transfer was not of interest in this investigation.

The flow being modeled is swirling and in such turbulent flows viscosity is typically anisotropic, so the most reliable turbulence model Reynolds Stress Model (RSM) was chosen [11], [18]. The RSM closes the Reynolds-averaged Navier-Stokes equations by solving transport equations for the Reynolds stresses, together with an equation for the dissipation rate. This means that seven additional transport equations are required in 3D flows. Since the RSM accounts for the effects of streamline curvature, swirl, rotation, and rapid changes in strain rate in a more rigorous manner than one-equation and two-equation models, it has greater potential to give accurate predictions for complex flows [19]. The transport equations for the transport of the Reynolds Stresses are referred to [18] and [20].

D. Simulation Set-Up

Material

Simulations were carried out with single-phase water, and the flow was assumed to be steady and isothermal. The water density and viscosity were specified as 998.2kgm^{-3} and 1.003×10^{-3} kgm^{-1}s^{-1}.

Boundary Conditions

At the inlet, a velocity inlet boundary condition was used. The turbulence was specified in terms of intensity and hydraulic diameter at both the inlet and outlet. The turbulence intensity is defined as the ratio of the root-mean-square of the velocity fluctuations to the mean velocity. It was calculated from [16]:

$$I=0.16\times(Re)^{-1/8},\ Re=(U\times D\times\rho)/\mu \quad (4)$$

where Re is the Reynolds number, U is the average velocity, ρ is the density, and μ is the viscosity. A series of simulations were carried out with inlet velocities being 1m/s, 2m/s and 3m/s.

A pressure outlet boundary condition was imposed at the outlet of the computational model. This boundary condition results in a better rate of convergence when backflow occurs during iteration.

The pipe walls were specified as being stationary and no slip walls to match the simulation conditions. Wall roughness was modelled by specifying the roughness height, Ks, as 1.5 x 10^{-05}m. This value is so small that the walls can be considered to be hydraulically smooth. The Non-Equilibrium wall functions were applied in the near wall region.

Solver

Pressure-based Segregated Solver was chosen for the steady state simulation. Absolute velocity formulation was used.

Solution Methods

The SIMPLE discretization technique was applied for the pressure-velocity coupling. A second order upwind scheme was employed for viscous terms.

Convergence Criterion

The convergence criterion used for all cases was that the scaled residuals of x, y, z velocities, k, and ε, and Reynolds stresses have decreased by four orders of magnitude. The mass flow rate at the outlet was also monitored and the solution was deemed to have reached a steady state when this parameter achieved a constant value over a large number of iterations.

V. Results and Discussions

A. Pressure Drop

The pressure loss across the lobed swirl pipe itself is greater than circular pipe due to the additional turbulence generated through artificial roughness of the non-circular pipe surfaces [12], [13]; the energy lost is partly converted into angular momentum of swirling flow. Fig. 7 demonstrates the pressure drop within the 600mm and 400mm length swirl pipes with the inlet velocities being 3m/s, 2m/s, and 1m/s respectively. From Fig. 7, a larger inlet velocity causes larger pressure drop in both the 100+400+100 swirl pipe and the 100+200+100 swirl pipe. From Table I, For the three inlet velocities, the

overall pressure drop caused by the 100+400+100 swirl pipe is larger than the 100+200+100 swirl pipe due to its larger contact area with fluid thus pipe friction and the differences in pressure drop are more obvious in flows with higher velocities.

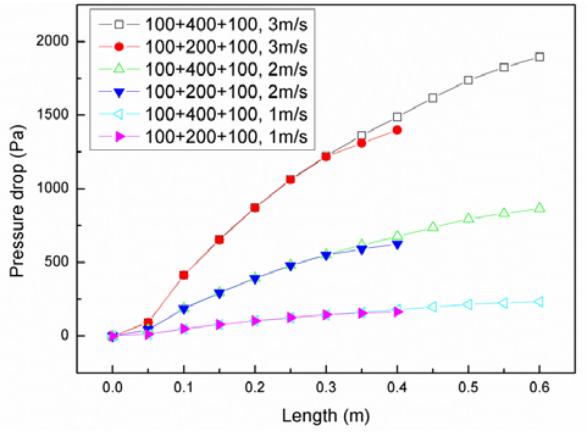

Fig. 7 Pressure drop across the two swirl pipes in flows with various inlet velocities

TABLE I
COMPARISON OF THE TWO SWIRL PIPES ON PRESSURE DROP AND TANGENTIAL VELOCITY

Velocity (m/s)	Pressure drop (Pascal)		Final tangential velocity (m/s)	
	600mm swirl pipe	400mm swirl pipe	600mm swirl pipe	400mm swirl pipe
1	233.24	165.25	0.151	0.156
2	866.2	625.86	0.33	0.345
3	1894.99	1399.5	0.545	0.555

B. Swirl Development within Swirl Pipe

The swirl pipe adds a rotating momentum to the flow within itself and direct to the circular pipe downstream of it, turning the fluid clockwise in addition to the axial velocity along the pipe. The velocity component, which mainly affects the swirl flow field, is the tangential velocity component, which has a distribution dependent on the swirl generation mechanism [11]. Fig. 8 shows the development of tangential velocity within the 100+400+100 swirl pipe and 100+200+100 swirl pipe for the three inlet velocities of 3m/s, 2m/s and 1m/s. It is clear that both the two swirl pipes induce larger tangential velocity in flows with higher velocities. For the three inlet velocities and for the 100+400+100 swirl pipe, a sharper tangential velocity increase is seen from the middle of the entry transition pipe (0.05m in the horizontal axis) and it reaches the highest value in the middle of the 400mm swirl inducing pipe (0.3m in the horizontal axis); the tangential velocity decreases slightly in the second half of the swirl inducing pipe indicating that it is acting as a constraint to the induced tangential velocity. While in the case of 100+200+100 swirl pipe, the whole 200mm swirl inducing pipe contributes to the tangential velocity development as it can be seen that the largest value appears at the joint of swirl inducing pipe to the exit transition pipe with this largest values are almost identical in the two swirl pipes. In both the two swirl pipes, exit transition pipe causes a decrease in tangential velocity. However, the final tangential velocity at the exit of the 100+200+100 swirl pipe is slightly larger than that of the 100+400+100 swirl pipe in flows with the three different inlet velocities.

Fig. 9 shows the variation of swirl intensity within the two swirl pipes for the three velocities. Generally, in both the 100+400+100 and 100+200+100 swirl pipe, the first 0.3m length of the swirl pipes contribute to swirl induction with the swirl intensity value and its variation trend are almost identical. In the rest of the swirl pipes (0.3~0.6m for the 600mm swirl pipe and 0.3~0.4 for the 400mm swirl pipe), decrease in swirl intensity are observed in both the swirl pipes, however, the final swirl intensity downstream of 100+200+100 swirl pipe is slightly higher than that of the 100+400+100 swirl pipe. The detailed initial swirl intensity downstream of both the swirl pipes for the three velocities is listed in Table II.

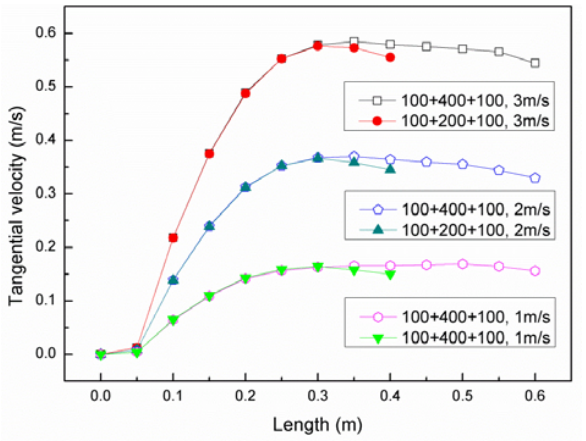

Fig. 8 Tangential velocity distribution within the two swirl pipes for various inlet velocities

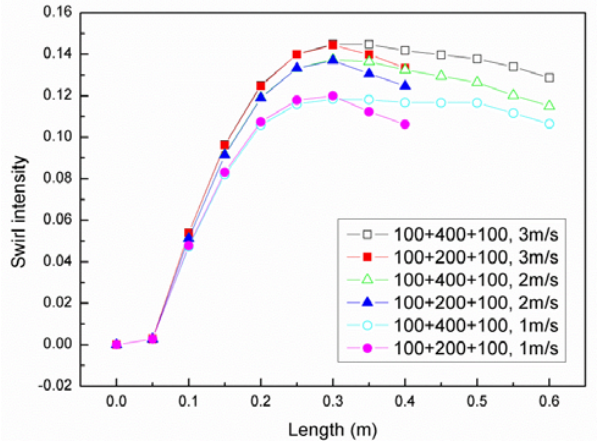

Fig. 9 Swirl intensity distribution within the two swirl pipes for various inlet velocities

TABLE II
COMPARISON OF THE TWO SWIRL PIPES ON SWIRL INTENSITY AND SWIRL EFFECTIVENESS

Velocity (m/s)	Final swirl intensity		Swirl effectiveness	
	600mm swirl pipe	400mm swirl pipe	600mm swirl pipe	400mm swirl pipe
1	0.106	0.106	0.228	0.321
2	0.115	0.125	0.265	0.398
3	0.129	0.133	0.305	0.428

C. Swirl Effectiveness

Fig. 10 shows the swirl effectiveness variation within the 100+400+100 and 100+200+100 swirl pipe with three different inlet velocities. In the entry transition pipe for all three conditions, there is a quick increase in swirl effectiveness. This is because the gradual transition from circular cross-section to the lobed geometry reduces frictional losses from the pipe walls thereby producing a more effective swirl induction in the expense of a smaller pressure drop. The quick increase in tangential velocity is further continued within the swirl inducing pipe that it is immediately adjacent to the entry transition pipe where the swirl effectiveness reaches its highest value in this duration (0.1~0.15m). Afterward, the increase in tangential velocity slows down till the tangential velocity reaches the maximum value in 0.3m in the horizontal axis as shown in Fig. 8. In this duration, swirl inducing pipe still contributes to swirl induction despite of the negative slope in swirl effectiveness. After the point of 0.3m, the second half of the swirl inducing pipe and the exit transition pipe of the 100+400+100 swirl pipe is restricting the tangential velocity that has been generated. However, only the exit transition pipe of the 100+200+100 swirl pipe is restricting the tangential velocity thus the overall swirl effectiveness of the 100+200+100 swirl pipe is larger than the 100+400+100 swirl pipe. It is also clear from Fig. 10 that swirl effectiveness of the two swirl pipe is larger in flows with higher velocities. A detailed swirl effectiveness value for the two swirl pipes in the three conditions is referred to Table II.

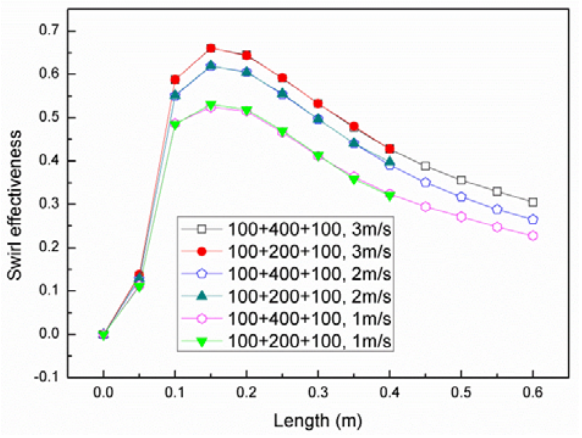

Fig. 10 Swirl effectiveness variation within the two swirl pipes for various inlet velocities

D. Swirl Decay

The induced swirl flow decayed with increasing distance downstream the swirl pipe and reverted back to the upstream flow profile at different distances downstream according to the inlet velocities. The decay of swirl is caused by the transport of angular momentum to the pipe wall. Fig. 11 depicts the average tangential velocity distribution downstream of both the 100+400+100 swirl pipe and the 100+200+100 swirl pipe for inlet velocities of 3m/s, 2m/s and 1m/s. It is clear for both the two swirl pipes that tangential velocity decreases with increasing distance downstream and finally decreases to zero where the swirl effect fades away. It is also clear that the effectiveness of both the two swirl pipes is more prominent for flows with larger velocities. However, for the same inlet velocities, the initial tangential velocities downstream of 100+200+100 swirl pipe and along the circular pipe are slightly larger than that of when 100+400+100 swirl pipe is used, this is even true in flows with a larger velocity.

Fig. 12 presents the swirl intensity calculated at swirl pipe exit and planes downstream of the two swirl pipe exits. It is clear for both the two pipes that swirl intensity decreases with increasing distance downstream of the swirl pipe exit with larger swirl intensity observed both at the swirl pipe exit and downstream of it in flows with higher velocities (Reynolds number). The swirl decay rate is in good agreement with exponential trend with the decay rate of swirl flow induced by 100+400+100 swirl pipe in flows with inlet velocity of 3m/s, 2m/s and 1m/s being 0.0332, 0.0356, and 0.0398 while the decay rate for 100+200+100 swirl pipe are 0.0328, 0.0349 and 0.0398. It is clear that, for the inlet velocity of 2m/s and 3m/s, 100+200+100 swirl pipe has a superior swirl induction effect as it induces larger initial swirl intensity downstream and has a smaller swirl decay rate than when 100+400+100 swirl pipe is used. However, for the inlet velocity of 1m/s, the advantage of 100+200+100 swirl pipe is negligible.

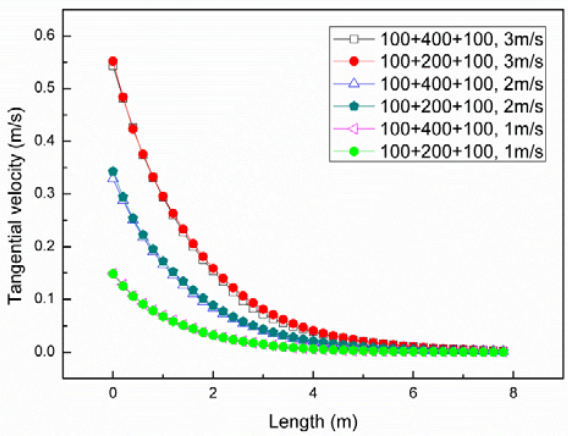

Fig. 11 Tangential velocity distribution downstream of the two swirl pipes for various inlet velocities

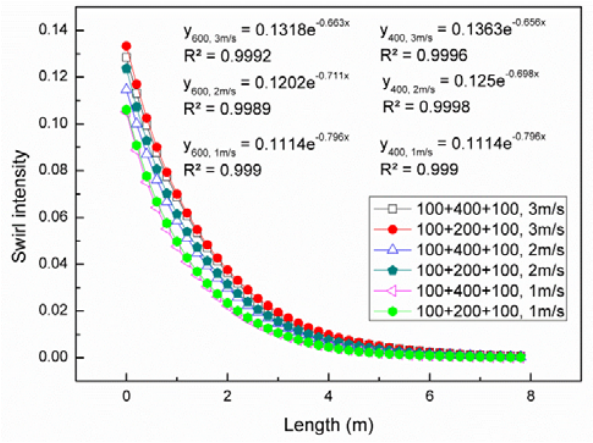

Fig. 12 Swirl intensity variation downstream of the two swirl pipes for various inlet velocities

E. Wall Shear Stress

The effects of the two swirl pipes on increasing shear stress at the pipe surface are also investigated and compared as we intend to apply this swirl pipe into Clean-In-Place procedures, in which the wall shear stress was reported to be the local tangential force acting on the soil on the surface and remove them [21].

The shear stress, for a Newtonian fluid, is defined by the normal velocity gradient at the wall as: $\tau_w = \mu \frac{\partial u}{\partial y}$, where μ is dynamic viscosity of the fluid, u is velocity of the fluid along the boundary and y is height above the boundary. For swirl flow, angular momentum is transported into the pipe wall, generating a sharp tangential velocity gradient in the wall. It is expected this tangential velocity gradient will induce tangential wall shear stress acting on the pipe surface in addition to the axial wall shear stress that is parallel to the straight circular pipe.

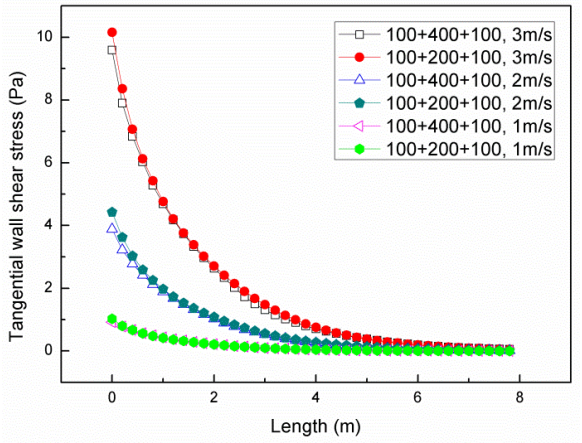

Fig. 13 Tangential wall shear stress distribution downstream of the two swirl pipes for various inlet velocities

From Fig. 13, it is clear that flow passing through both the two swirl pipes will generate tangential shear stress at the wall and direct to the downstream. The tangential shear stress will decay and finally fades away with a similar variation trend of tangential velocity as shown in Fig. 11, which suggests that tangential wall shear stress is closely associated with tangential velocity thus swirl intensity. It can be noticed that an increase of inlet velocity from 1 m/s to 3 m/s causes a sharp rise in tangential wall shear stress downstream of the two swirl pipes; this may suggest that the effect of the swirl pipe on tangential shear stress is more prominent in flows with a higher Reynolds number.

It is also clear from Fig. 13 that the initial tangential wall shear stress and the values downstream of the 100+200+100 swirl pipe are slightly larger than that of 100+400+100 swirl pipe and this is clearer in flows with larger inlet velocities.

Fig. 14 depicts the average non-dimensional tangential wall shear stress along the pipe downstream of the two swirl pipe exits for various inlet velocities. It shows that the trend of variation for non-dimensional tangential wall shear stress is similar to that of swirl intensity as shown in Fig. 12. This further indicates that the presence and variation of tangential wall shear stress is mainly dependent on swirl intensity. One again, the 100+200+100 swirl pipe is slightly better in increasing non-dimensional tangential wall shear stress than the 100+400+100 swirl pipe due to the relatively larger swirl intensity induced.

Fig. 15 presents the average axial wall shear stress downstream of the two swirl pipe exits for various inlet velocities. It shows that the two swirl pipes also has the effect of increasing axial wall shear stress downstream them but in a very slight way and lasts for a short distance compared with tangential wall shear stress. The effect of the swirl pipes on axial wall shear becomes less obvious with decreasing inlet velocity (Reynolds number). Their effect is almost negligible for flows with an inlet velocity of 1 m/s. with the same inlet velocities, 100+200+100 swirl pipe induces a slightly higher axial wall shear stress increase than that of 100+400+100 swirl pipe, however, its advantage stops being obvious in flows with lower velocities.

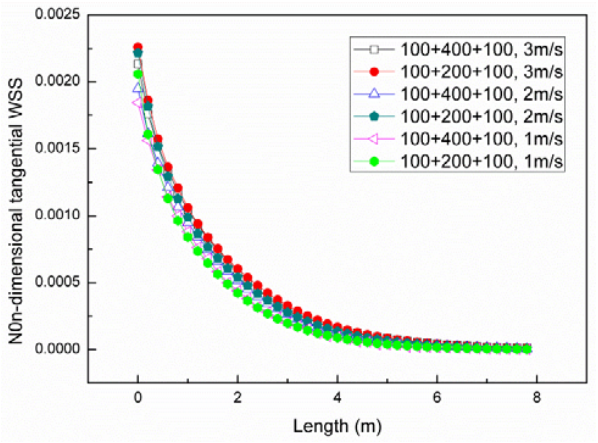

Fig. 14 Non-dimensional tangential WSS distribution downstream of the two swirl pipes for various inlet velocities

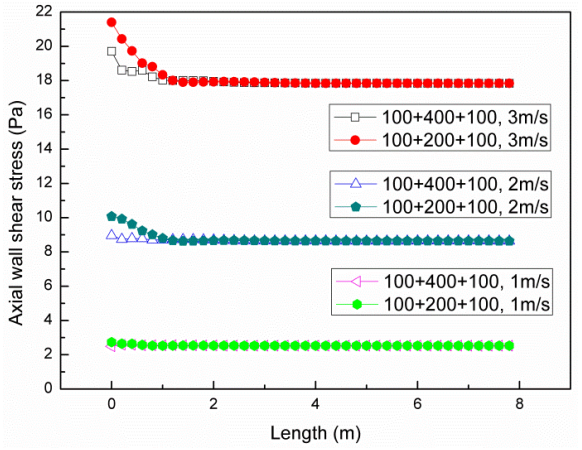

Fig. 15 Axial wall shear stress distribution downstream of the two swirl pipes for various inlet velocities

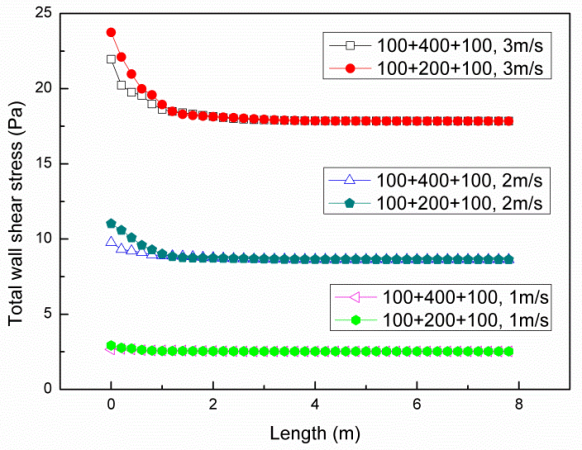

Fig. 16 Total wall shear stress distribution downstream of the two swirl pipes for various inlet velocities

Fig. 16 shows the total wall shear stress downstream of the two swirl pipes, which is the combined action of the tangential and axial shear stress component acting on the pipe surface. It is clear that swirl pipes locally increases mean wall shear stress downstream of it, with the increased value and effective distance more remarkable for a faster inlet flow velocity (a large Reynolds number and large swirl intensity). For a flow velocity of 3m/s which is typically the velocity of cleaning fluid circulating in a Clean-In-Place procedure, 100+400+100 swirl pipe raises mean shear stress at the wall from 17.8 Pascal prior swirl pipe inlet to 22 Pascal (23.5% increase) just downstream of it. The wall shear stress decays in accordance with swirl intensity, and in the point 1m (20D) downstream swirl pipe exit the increase in wall shear stress is 5%. While the 100+200+100 swirl pipe rises wall shear stress from 17.8 Pascal before it to 23.7 Pascal (33.1% increase) downstream of it and maintains at least 5% increase in mean wall shear stress in the position 1.1m (22D) downstream of it .Therefore, it can be concluded that 100+200+100 swirl pipe is better in increasing and maintaining wall shear stress downstream it than that of 100+400+100 swirl pipe. The advantage of 100+200+100 swirl pipe on increasing total wall shear stress is more obvious in flows with larger velocities, which is typically the velocity used in the CIP procedures.

VI. Conclusions

In this study, the ability of two swirl pipes in terms of inducing swirl into flows passing through them have been numerically investigated and compared. The objective has been the prediction and comparisons of pressure drop and tangential velocity caused by the two swirl pipes, the swirl intensity and its decay law downstream of the two swirl pipes, the swirl effectiveness of the two swirl pipes and their effects on increasing the wall shear stress downstream of them. The following results have been obtained:

- The overall pressure drop caused by the 100+400+100 swirl pipe is larger than the 100+200+100 swirl pipe for the same inlet velocities and the pressure drop increases with increasing inlet velocities.
- For the 100+400+100 swirl pipe, the entry transition pipe and the first half of the swirl inducing pipe contribute to swirl development, the second half of swirl inducing pipe and the exit transition pipe act as a constraint to the induced swirl. While within the 100+200+100 swirl pipe, only the exit transition pipe constrains the induced swirl. The final tangential velocity and the swirl intensity just downstream of the 100+200+100 swirl pipe for various inlet velocities are slightly larger than that of 100+400+100 swirl pipe.
- The overall swirl induction effectiveness of the 100+200+100 swirl pipe is larger than that of the 100+400+100 swirl pipe.
- The induced tangential velocity, swirl intensity and the effective distances are slightly larger downstream of the 100+200+100 swirl pipe than when 100+400+100 swirl pipe is used with its advantage is more true in flows with larger Reynolds Number.
- Swirl pipes impose a tangential wall shear stress within itself and direct to downstream with its value and variation trend being dependent on swirl intensity. The induced tangential wall shear stress after the 100+200+100 swirl pipe is slightly larger than when 100+400+100 swirl pipe is used due to the relatively larger swirl intensity.
- The axial and total wall shear stress are also slightly larger downstream of the 100+200+100 swirl pipe than that of the 100+400+100 swirl pipe with its advantage being more true in flows with a larger inlet velocity.
- The 100+200+100 swirl pipe ismore cost-effective in swirl induction and is better in maintaining the wall shear stress increase downstream it than that of 100+400+100 swirl pipe.

From the simulation results, 100+200+100 swirl pipe induce slightly stronger swirl into flows passing through it and also lasts for slightly longer distance than that of 100+400+100 swirl pipe in the expense of a smaller pressure loss. It is also clear that the 100+200+100 swirl pipe is more

cost effective in increasing wall shear stress downstream of it than when a 100+400+100 swirl pipe, thus it should results in better performance when applied in the Clean-In-Place procedures in the pipe cleaning system.

REFERENCES

[1] Leliévre, C., et al., Cleaning in place: effect of local wall shear stress variation on bacterial removal from stainless steel equipment. Chemical Engineering Science, 2002. 57: p. 1287-1297.
[2] Jensen, B. B. B., et al., Local Wall Shear Stress Variations Predicted by Computational Fluid Dynamics for Hygienic Design. Food and Bioproducts Processing, 2005. 83(1): p. 53-60.
[3] Gillham, C. R., et al., Cleaning-in-Place of Whey Protein Fouling Deposits. Food and Bioproducts Processing, 1999. 77(2): p. 127-136.
[4] Dev, S. R. S., et al., Optimization and modeling of an electrolyzed oxidizing water based Clean-In-Place technique for farm milking systems using a pilot-scale milking system. Journal of Food Engineering, 2014. 135(0): p. 1-10.
[5] Pathogen Combat, E.I.P., Factors affecting fouling and cleanability of closed food contact surface. 2011.
[6] Lelieveld, H. L. M., Mostert, M.A., Holah, J. and White, B., Hygiene in Food Processing. Vol. 1st edn. 2003, Woodhead, Cambridge, UK.
[7] Changani, S. D., M. T. Belmar-Beiny, and P. J. Fryer, Engineering and chemical factors associated with fouling and cleaning in milk processing. Experimental Thermal and Fluid Science, 1997. 14: p. 392-406.
[8] Sharma, M. M., et al., Factors Controlling the Hydrodynamic Detachment of Particles from Surfaces. Journal of Colloid and Interface Science, 1991. 149: p. 121-134.
[9] Hwang, Y. K. and N. S. Woo, Wall Shear Stress in the Helical Annular Flow with Rotating Inner Cylinder. Diffusion and Defect Data Part B Solid State Phenomena, 2007. 120: p. 261-266.
[10] Li, G., et al., Improving the efficiency of 'Clean-In-Place' procedures using a four-lobed swirl pipe: A numerical investigation. Computers & Fluids, 2015. 108(0): p. 116-128.
[11] Najafi, A. F., S. M. Mousavian, and K. Amini, Numerical investigations on swirl intensity decay rate for turbulent swirling flow in a fixed pipe. International Journal of Mechanical Sciences, 2011. 53(10): p. 801-811.
[12] Ganeshalingam, J., Swirl Induction for Improved Solid-Liquid Flow in Pipes. 2002, University of Nottingham.
[13] Ariyaratne, C., Design and Optimisation of Swirl Pipes and Transition Geometries for Slurry Transport, in School of Chemical, Environmental and Mining Engineering. 2005, University of Nottingham.
[14] Kitoh, O., Experimental study of turbulent swirling flow in a straight pipe. Journal of Fluid Mechanics, 1991. 225: p. 445-479.
[15] Steenbergen, W. and J. Voskamp, The rate of decay of swirl in turbulent pipe flow. Flow measurement and instrumentation, 1998. 9: p. 67-78.
[16] ANSYS, I., ANSYS Fluent 14.0 User's Guide. 2011: Southpointe, Canonsburg, PA, USA.
[17] Bakker, A., Boundary Layers and separation, in Applied Computational Fluid Dynamics. 2002.
[18] Fokeer, S., I.S. Lowndes, and D.M. Hargreaves, Numerical modelling of swirl flow induced by a three-lobed helical pipe. Chemical Engineering and Processing: Process Intensification, 2010. 49(5): p. 536-546.
[19] ANSYS, I., ANSYS Fluent 14.0 Theory Guide. 2011: Southpointe, Canonsburg, PA, USA.
[20] Speziale, C.G., S. Sarkar, and T. B. Gatski, Modelling the Pressure-Strain Correlation of Turbulence: An Invariant Dynamical Systems Approach. J. Fluid Mech, 1991. 227: p. 245-272.
[21] Jensen, B.B.B., M. Stenby, and D.F. Nielsen, Improving the cleaning effect by changing average velocity. Trends in Food Science & Technology, 2007. 18: p. S58-S63.